

Be Careful with Rotation: A Uniform Backdoor Pattern for 3D Shape

Linkun Fan, Fazhi He *, Qing Guo, Wei Tang, Xiaolin Hong, Bing Li *

Abstract—For saving cost, many deep neural networks (DNNs) are trained on third-party datasets downloaded from internet, which enables attacker to implant backdoor into DNNs. In 2D domain, inherent structures of different image formats are similar. Hence, backdoor attack designed for one image format will suite for others. However, when it comes to 3D world, there is a huge disparity among different 3D data structures. As a result, backdoor pattern designed for one certain 3D data structure will be disable for other data structures of the same 3D scene. Therefore, this paper designs a uniform backdoor pattern: *NRBdoor* (**Noisy Rotation Backdoor**) which is able to adapt for heterogeneous 3D data structures. Specifically, we start from the unit rotation and then search for the optimal pattern by noise generation and selection process. The proposed *NRBdoor* is natural and imperceptible, since rotation is a common operation which usually contains noise due to both the miss match between a pair of points and the sensor calibration error for real-world 3D scene. Extensive experiments on 3D mesh and point cloud show that the proposed *NRBdoor* achieves state-of-the-art performance, with negligible shape variation.

Index Terms—Backdoor Attack, 3D Mesh, Point Cloud, Deep Neural Network, Uniform Backdoor Pattern.



1 INTRODUCTION

3D mesh and point cloud are the most popular structures to construct 3D scenes [1], [2], [3], [4], [5]. In detail, point cloud is more efficient since it is easy to be obtained and is close to raw data. By contrast, 3D mesh requires less element to represent large shape and to capture details. However, due to the inherent irregularities, conventional DNN techniques designed for 2D image [6], [7], [8] cannot directly process 3D shape. Recently, many DNNs that extract and process with 3D feature were designed, such as MeshCNN [9], DiffusionNet [10] and SubdivNet [11] for 3D mesh, PointNet [12], DGCNN [13] and PointBert [14] for point cloud.

However, DNN has been proven be vulnerable due to poor interpretability and black-box character [15], [16], [17], [18]. Adversarial attack [19], [20], [21], [22], [23], [24] is a well-know method to deceive DNN in inference stage. Attacker crafts adversarial samples to mislead DNN by adding perturbation to clean samples, which is hardly detected by human vision [25], [26], [27]. In practical, most DNNs require huge data for training. To save cost, developers usually download third-party datasets from internet, instead of collecting data by themselves. Hence, this enables attackers to destroy DNN in training stage.

This paper focuses on one classical attack in the training stage which is called *backdoor attack*. A successful backdoor attack does not decrease the performance on clean data, yet is able to deceive DNN to make the targeted decision specified by the attacker. This kind of attacks in training phase has raised concerns for the development of DNNs in applications such as Virtual Reality (VR), Augmented Reality (AR) and self-driving [28], [29].

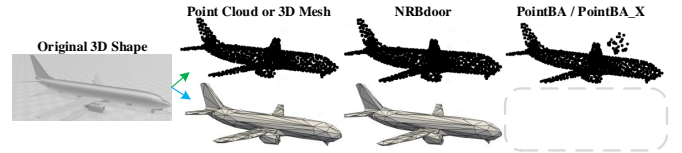


Fig. 1. *NRBdoor* is able to adapt for data structure variation (from point cloud to 3D mesh, for example) during implanting backdoor into 3D DNN. Meanwhile, *NRBdoor* is more natural than PointBA [30] and PointBA_X [31] which only focus on point cloud.

For one thing, typical backdoor patterns designed for 2D image [32], [33], [34], [35], [36], [37] are unsuitable for 3D shape, such as attaching portion or adding perturbation. This is mainly due to the data structure disparity between 2D image and 3D shape. For example, it is difficult to attach a patch into 3D mesh like in image domain, since the elements of 3D mesh are correlated to each other. Attaching patches may break the characteristic of manifold and watertight that most mesh DNNs require for.

For another thing, although there are many different 2D image formats, their inherent structures are similar, which are uniform 2D arrays of pixel values. Backdoor attack designed for one image format will suite for others. However, when it comes to 3D world, different 3D structures are discrepant. For instance, the data structure of 3D point cloud includes disperse points with geometric coronations. In contrary, the data structures of 3D meshes are heterogeneous, in which, a face is constructed with its neighbor edges, and a edge is constructed with its two end vertices. Therefore, vertices of 3D mesh include both geometric coronations and topology connection, and is different from point of 3D point cloud. As a result, the backdoor pattern designed for point cloud [30], [31] is usually not adaptable for 3D mesh.

Based on above analyses, we argue that the backdoor pattern for 3D shape should meet two requirements: 1) do

• The authors are with the School of Computer Science, Wuhan University, Hubei, China, 430072

* E-mail: fzhe@whu.edu.cn, bingli@whu.edu.cn

not change the correlation between different elements of 3D shape, 2) able to adapt for heterogeneous 3D data structure.

Therefore, this paper designs a uniform backdoor pattern for 3D shape: *NRBdoor* (Noisy Rotation Backdoor). Rotation is a common operation in 3D world. Movement of 3D sensor or 3D object will inevitably introduce rotation. Specifically, rotation matrix must be orthogonal matrix, which under the constraint of $R \cdot R^T = I$. However, due to the way to calculate rotation matrix and sensor calibration error, the actually used rotation matrix is usually non-orthogonal, which is called noise rotation matrix R_n in this paper. Hence, conducting noise rotation on 3D shape is a natural situation in 3D world.

This paper is the first work to address uniform backdoor pattern for heterogeneous 3D structures, and the first work to implant backdoor into mesh DNNs. The main contributions are as follows:

- A novel uniform backdoor pattern *NRBdoor* for 3D shape is proposed. *NRBdoor* is able to adapt for 3D data structures variation, during implanting backdoor into 3D shape DNN (3D DNN). Meanwhile, it is imperceptible and natural for real-world 3D applications.
- *NRBdoor* is the first backdoor pattern friendly to 3D mesh. It preserves the characteristic of manifold and watertight of 3D mesh, which are required by many mesh DNNs.
- Results on 3D mesh show that the attack success rate (ASR) for SOTA mesh DNNs (such as MeshCNN, SubdivNet, MeshWalker) on public datasets achieve 100% with BAc descend less than 0.5%. For 3D point cloud, ASR for SOTA point DNNs (PointNet, PointNet++ and DGCNN) are higher than 93%, under well stealthiness.
- At present, considering there is no baseline for defending backdoor attack on 3D shape, we propose Saliency-based Point cloud backdoor defense (SP-defense). It is able to decrease ASR of PointBA_X from 82% to 23%.

1.1 DNN for Point Cloud or 3D Mesh

3D point cloud and 3D mesh are both popular 3D data structures to represent 3D shape in modern researches and applications [38], [39]. Point cloud X is constituted by a set of n 3D points $X \rightarrow \{p_1, p_2, \dots, p_n\}$, and each point p_i is represented by 3D coordinates (x_i, y_i, z_i) . Meanwhile, 3D mesh with n vertex and m faces is defined by $X \rightarrow \{v_1, v_2, \dots, v_n; c_1, c_2, \dots, c_m\}$, where v_i is the i -th vertex with positions in $R^{n \times 3}$, and c_j is the j -th polygonal faces. 3D DNN $F(X, \theta) \rightarrow y$ aims to map an input 3D shape X to its corresponding class label $y \in Y$, under well-trained parameters θ . For ease of reading, this paper refers DNN designed for point cloud as point DNN and for mesh as mesh DNN.

Point DNN: PointNet [12] is the first point DNN to directly process point cloud. It learns a spatial encoding of each point and then aggregates all individual point features to a global point cloud signature. PointNet++ [40] achieves better results by considering hierarchical structure based on PointNet. DGCNN [13] is a typical convolution-based

point DNN, which transforms point cloud to a graph, and learns feature by the defined EdgeConv. PCT [41] designs a full attention mechanism, which enables each point to affect every other point in the point cloud. PointBert [14] designs a new pre-train method based on point cloud transformer. It achieves 93.8% accuracy on ModelNet40 for classification.

Mesh DNN: MeshCNN [9] considers that each edge is adjacent to two faces and four edges in manifold triangle mesh, and then defines an ordering invariant convolution to learn 3D feature. Instead of learning neighborhood information, MeshWalker [42] transforms 3D mesh to several edge sequences by walking along edges. Moreover, SubdivNet [11] designs a general mesh convolution using a mesh pyramid structure for effective feature aggregation, its key process is to remesh the input mesh to obtain loop subdivision sequence connectivity. DiffusionNet [10] learns feature from face by extending the Laplacian operator.

1.2 Backdoor Attack

In image domain, lots of backdoor attacks have been developed recently [43], [44], [45]. They are usually divided to poison-label backdoor attack and clean-label backdoor attack, based on whether label of poisoned sample is changed. In 3D domain, PointBA [30] and PointBA_X [31] are pioneers researching backdoor attack which follow the way developed in image domain and only focus on point cloud. PointBA defines a unified framework of 3D backdoor trigger implanting function and designs two backdoor patterns (a ball and clean rotation) under poison-label and clean-label situations. PointBA_X inserts a small cluster of points as backdoor pattern. The optimal spatial location and local geometry are searched by optimization. Meanwhile, [46] presents Poisoning MorphNet in a clean-label setting. Though the well performance on point cloud, they will be disable on 3D mesh since data structure disparity. Therefore, this paper designs *NRBdoor* to adapt for heterogeneous 3D data structure.

1.3 Isometrics Transformations

Isometrics transformations of $\mathbb{R}^{n \times n}$ is a function f that preserves euclidean distance:

$$\|f(x) - f(y)\| = \|x - y\| \quad \forall x, y \in \mathbb{R}^{n \times n} \quad (1)$$

The base operations of isometry are translation: $f(x) = x + a$ and identity rotation: $f(x) = Rx$. We don't consider translation in this paper, since it can be easily eliminated by normalization. By this way, we only conduct linear transformation (a transformation that fixes the origin) on 3D shape which is:

$$f(X) = RX = X' \quad \forall X, X' \in \mathbb{R}^{n \times n} \quad (2)$$

Here, R is an orthogonal matrix whose determinant equals to 1. The rotation matrices are defined as a subset of:

$$SO(n) = R \in \mathbb{R}^{n \times n} | RR^T = I, \det(R) = 1 \quad (3)$$

In detail, the Euler's rotation theorem claims that any rotation in \mathbb{R}^3 can be decomposed to three rotations around x, y, z axes:

$$R = R_{\theta_x} R_{\theta_y} R_{\theta_z} \quad (4)$$

1.4 Methods to Calculate Rotation Matrix

Perspective-n-Point (PnP) aims to solve the movement between 2D to 3D. The formal description is: given coordinates of n 3D points p^W in world coordinate system C^W and their corresponding coordinates p^P in pixel coordinate system C^P , PnP wants to search the pose (rotation R , and translation t) of camera in C^W [47]. The popular solutions include Direct Linear Transform(DLT), Perspective-Three-Point(P3P) [48], Efficient Perspective-n-Point(EPnP) [49] and Bundle Adjustment(BA) [50]. All these methods work based on correct match of 2D pixel and 3D point. However, in practical, miss match is a common scenes due to illumination variation, low resolution and fast movement. Therefore, the actually used rotation usually contains noise.

Iterative Closest Point(ICP) is a popular method to search the movement between 3D to 3D, which can be described as: given two 3D point sets $\mathcal{P}^1 : \{p_1^1, p_2^1, \dots, p_n^1\}$, $\mathcal{P}^2 : \{p_1^2, p_2^2, \dots, p_n^2\}$, ICP aims to find the optimal rotation R and translation t between \mathcal{P}^1 and \mathcal{P}^2 [51]. The main solving methods contain SVD decompose and BA [50]. For this kind of methods, the rotation noise mainly comes from miss match of 3D point pair and the error left by optimization.

2 PROBLEM FORMULATION

Attack Scenario: Our backdoor pattern is designed for the classical scenario that the developer trains his DNN on third-party datasets. Under this scenario, attacker can only manipulate the training datasets, but cannot changes the model, inference schedule and the training process.

Backdoor Attack Description: We define 3D DNN as $F(X, \theta) \rightarrow y$, which maps an input 3D shape X to its corresponding class label $y \in Y$ by learning parameter θ on training data D_{train} . The goal of attacker is to implant a backdoor into the victim 3D DNN by poisoning D_{train} , so that the victim 3D DNN will follow the attacker's malicious purpose. In inference stage, showing the certain pattern to the infected 3D DNN will activate the backdoor, which misleads it to output the target label y^t . The process to implant backdoor pattern is done by 1) design an appropriate backdoor pattern P , 2) generate poisoned samples by conducting P on partial training data, 3) inject poisoned samples to clean training data D_{train} to generate poison training data D_{train}^{poi} , 4) train victim 3D DNN on D_{train}^{poi} for implanting backdoor. So that, clean model $F(X, \theta)$ is infected to poisoned model $F(X, \theta^{poi})$. Furthermore, poisoned testing dataset D_{test}^{poi} is generated to evaluate backdoor pattern.

Noise level γ : Stealthiness is a crucial factor to evaluate the probability that a backdoor pattern is detected by defender. We newly define a metrics to evaluate perturbation level called as rotation noisy level γ :

$$\gamma = \sum_{j=0}^3 \sum_{i=0}^3 ((R_n[i, j] - I[i, j])) \quad (5)$$

Here, γ indicates the distance between R_n and I , i, j mean the index of element in matrix, I is unit matrix. Note that, there are multiple R_n under certain γ .

3 NOISE ROTATION BACKDOOR PATTERN

A well-designed backdoor pattern achieves high attack success rate with as little perturbation as possible, and keeps the reduction of benign accuracy be small at the same time. It is reasonable that bigger shape variation will be easier implanted, but will result in weak stealthiness, vice versa. Therefore, there is a trade-off between ASR and stealthiness. In this paper, we aim to search for a noisy rotation R_n as the optimal trade-off, which can be formally described as:

$$R_n = \arg \max_{R_n} (Q_a(\mathcal{X}^{poi}) + Q_s(\mathcal{X}) + \frac{1}{\gamma}) \quad (6)$$

Here, $Q_a(\mathcal{X}^{poi})$ measures whether backdoor attacker can successfully achieve their malicious purposes when predicting poisoned samples \mathcal{X}^{poi} . $Q_s(\mathcal{X})$ measures whether the infected model be able to correctly predict benign samples \mathcal{X} :

$$Q_a(\mathcal{X}^{poi}) = \mathbb{E}_{(x,y) \sim \mathcal{P}_D} \mathbb{I}\{F(R \cdot X, \theta^{poi}) = y^t\} \quad (7)$$

$$Q_s(\mathcal{X}) = \mathbb{E}_{(x,y) \sim \mathcal{P}_D} \mathbb{I}\{F(X, \theta^{poi}) = y\} \quad (8)$$

Where, y^t is the targeted label. $F(\cdot, \theta^{poi})$ is the predicted class of 3D DNN under poisoned parameters θ^{poi} . \mathcal{P}_D is the distribution behind D and $\mathbb{I}(\cdot)$ is the indicator function. $\mathbb{I}(A) = 1$ if and only if the event ' A ' is true. $(R \cdot X) \in \mathcal{X}^{poi}$ means poisoned testing samples, and $X \in \mathcal{X}$ means benign testing samples.

The common way for solving equation (6) is to build Lagrangian, and then to search for the optimal by SGD. However, the gradient $\frac{\partial F(G(R_n \cdot X))}{\partial R_n}$ that classifier $F(\cdot)$ w.r.t rotation R_n is usually unavailable, since feature transformation function $G(X)$ is not continuous. Another way for searching optimal R_n is meta-heuristic algorithm such as PSO, GWO, et.al. But the calculation of fitness is time consuming, since it contains total training-testing process.

Aiming at searching optimal R_n efficiently, we shrink the searching space by fixing noise γ . Meanwhile, considering unit matrix I is the smallest rotation which will introduce zero shape variation and implant none backdoor, we start from the unit matrix I to find the optimal R_n . In detail, R_n is firstly divided into $R_n = N + I$ which includes noise N and unit matrix I . By doing so, our target becomes searching for noise N instead of noisy rotation R_n . Then we fix the rotation noise level γ and generate several noises N_{cand} by determining each element according to the given probability Pr . After that, we choose the optimal noise N_{cand} to obtain the final $R_n = N + I$ and the poisoned training data D_{train}^{poi} . R_n will be implanted into 3D DNN after trained on D_{train}^{poi} . Therefore, equation (6) and (7) are redefined as:

$$N = \arg \max_N (Q_a(\mathcal{X}^{poi}) + Q_s(\mathcal{X})) \quad s.t. \gamma = n \quad (9)$$

$$Q_a(\mathcal{X}^{poi}) = \mathbb{E}_{(x,y) \sim \mathcal{P}_D} \mathbb{I}\{F((N + I) \cdot x, \theta^{poi}) = y^t\} \quad (10)$$

The search process is done by **Noises Generation** and **Noise Selection**, shown as Algorithm 1. Meanwhile, the outline for implanting *BRBdoor* into 3D DNN is exhibited as Fig 2.

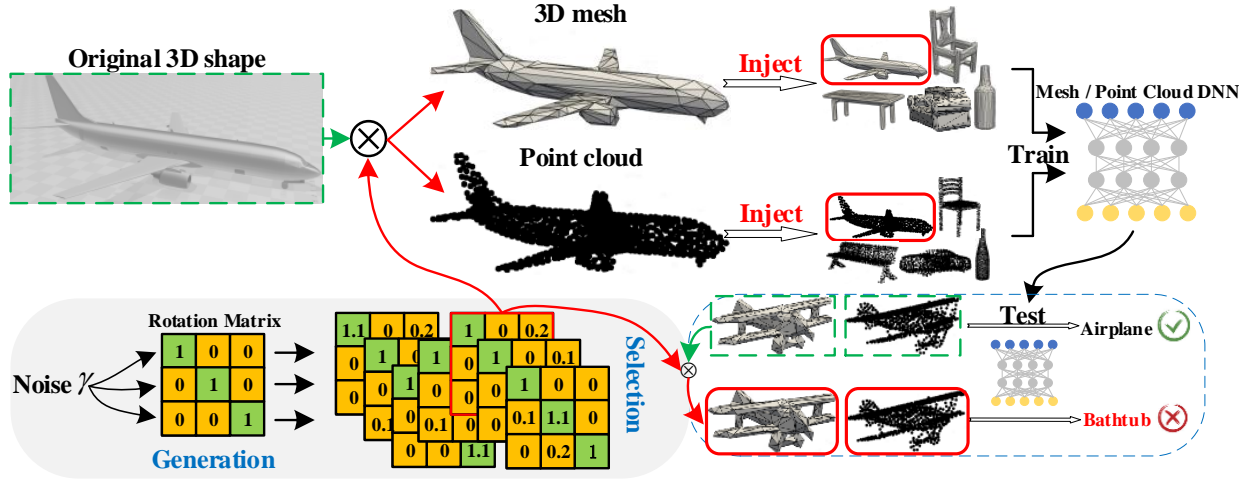


Fig. 2. Outline of backdoor attack by *NRBdoor*. *NRBdoor* is generated and selected by specifying data structure and victim 3D DNN. Then, 3D samples infected by *NRBdoor* were injected into D_{train} to obtain D_{train}^{poi} . 3D DNN will be deceived once *NRBdoor* appears after trained on D_{train}^{poi} .

Candidate Noises Generation: Given the rotation noise level γ , we set the precision to 0.1, and divide γ into $n_\gamma = \gamma/0.1$ number of unit noise N_u . The candidate noises are generated by distributing N_u to zero matrix M_0 , $N_{cand} = dis(N_u, M_0)$. Hence, there are 9^{n_γ} possible N_{cand} . Moreover, we have known that adding noise to different element of rotation matrix will introduce different shape variation. For example, noising diagonal elements will cause scaling, and noising off-diagonal elements will introduce additional rotation, shear and reflection. Since scaling is a common operation during feature transformation, scaling 3D shape will hardly be learned by 3D DNN. Therefore, the optimal noise tends to be found by noising off-diagonal elements of rotation matrix. To generate high quality N_{cand} , and preserve diversity, we assign a binary possibility Pr to guide the N_u distribution. After that, we distribute $n_\gamma N_u$ to each element of zero matrix M_0 according to their possibility for M times to generate candidate noises set \mathcal{N} .

Noise Selection: It is obvious that each candidate noise N_{cand} performs differently. Here, we maintain a score vector to evaluate the candidate noises N_{cand} . The selection process includes four steps: 1) initialize a zero vector as the initial score vector S , whose element represents the performance of each candidate noise. 2) randomly select one candidate noises N_{cand} from \mathcal{N} and samples X_{train} of percent α from D_{train} , and then conduct candidate noises N_{cand} on samples X_{train} by $X_{train}^{poi} = (N_{cand} + I) \cdot X_{train}$. Meanwhile, their labels are changed into y^t . The poisoned training dataset D_{train}^{poi} is generated by injecting X_{train}^{poi} to D_{train} . 3) score the candidate noise N_{cand} by training $F(\cdot)$ on D_{train}^{poi} and testing on poisoned testing dataset D_{test}^{poi} . Note that, an appropriate noisy rotation pattern will be learned by $F(\cdot)$ in a short time because of its unique feature from other classes. Therefore, in training stage, the model is trained in a small steps instead of full steps. 4) By repeating 2) and 3) for K times, the candidate noise N_{cand} with the highest score will be selected as the optimal noise N^{opt} . Finally, *NRBdoor* is acquired by $R_n^{opt} = N^{opt} + I$.

Conducting R_n : For 3D mesh and point cloud, we fix the correlation of each element and only move its points

Algorithm 1 Rotation Noises Generation and Selection

Input: Victim 3D point cloud classifier DNN $F(\cdot)$, 3D shape training dataset D_{train} , Noise level γ , Iteration times K , Candidate noises number M , Poison rate α

Output: *NRBdoor*

- 1: **Describe:** Generate candidate noises $\mathcal{N}_{(M \times 1)}$
- 2: Divide γ into $n_\gamma = \frac{\gamma}{0.1}$ number of $N_u_{(1 \times 1)}$
- 3: Determine probability $Pr_{(3 \times 3)}$
- 4: **for** $m \leq M$ **do**
- 5: $M_0 = zero_{(3 \times 3)}$
- 6: **for** $s \leq n_\gamma$ **do**
- 7: **if** $Pr[i, j] < rand(0, 1) < Pr[i + 1, j + 1]$ **then**
- 8: $M_0[i, j] + = N_u$
- 9: $\mathcal{N} \leftarrow N_{cand} = M_0$
- 10: **Describe:** Select noises
- 11: Initialize score vector $S_{(M \times 1)}$
- 12: **for** $k \leq K$ **do**
- 13: Randomly select $N_{cand} \in \mathcal{N}$, $X_{train} \in (D_{train} \cdot \alpha)$
- 14: $D_{train}^{poi} \leftarrow X_{train}^{poi} = (N_{cand} + I) \cdot X_{train}$
- 15: Inject D_{train}^{poi} into $D_{train} \rightarrow D_{train}^{poi}$
- 16: Train $F(\cdot)$ on D_{train}^{poi} by a small steps
- 17: Update score of N_{cand} by equation (10)
- 18: **return** $\mathcal{N}[argmax(S)] + I$

coordinate by R_n to acquire poisoned sample X^{poi} :

$$p_i^{poi} = R_n \cdot p_i \quad s.t. p_i \in X, p_i^{poi} \in X^{poi} \quad (11)$$

Implanting *NRBdoor*: We conduct R_n^{opt} on α percent samples of D_{train} to obtain poisoned training data D_{train}^{poi} . Meanwhile, labels of the poisoned samples are changed to the target label y^t . The mapping from *NRBdoor* to y^t will be implanted into the victim 3D DNN after training on D_{train}^{poi} .

4 EXPERIMENTS

We conduct extensive experiments to evaluate the performance of *NRBdoor* on 3D mesh and point cloud.

4.1 Experiment Setting

Datasets and Victim 3D DNNs: For 3D mesh, we choose Cubes [9], Manifold40 [11], and Shrec16 [52] as the evaluating datasets. In detail, Cubes contains 4381 meshes for 22 classes with 3722 for training and 659 for testing. Manifold40 is reconstructed by SubdivNet [11] based on ModelNet40. The author fixes the meshes which are not watertight in ModelNet40. There are 12311 meshes contained in Manifold40 for 40 classes, where 9,843 are used for training and the other 2,468 for testing. Shrec16 is a commonly used 3D mesh dataset which includes 30 classes, and each class contains 16 meshes for training and 4 meshes for testing. 3D meshes in the three datasets all contain 500 faces and are scaled into a unit cube. The victim mesh DNNs are various, including MeshCNN [9], MeshNet [53], SubdivNet [11], MeshWalker [42] and DiffusionNet [10]. Note that, it is infeasible to conduct every victim mesh DNN on the three datasets due to the structure restrictions. Therefore, we evaluate three victims on each dataset.

For point cloud, ModelNet40 [54] is chosen as the evaluating dataset. We uniformly sample 1,024 points from the surface of each object and rescale them into a unit cube. At the same time, PointNet [12], PointNet++ [12] and DGCNN [13] are chosen as the victim point DNNs. They are typical and are widely used to evaluate adversarial attack performance.

Evaluation Metrics: There are three metrics to evaluate backdoor pattern performance: Attack Success Rate(ASR), Benign Accuracy(BAc), and Stealthiness. In detail, ASR evaluates the ability to mislead DNN to output target class y^t , when the poisoned samples are shown. BAc is the accuracy of testing for infected DNN on clean samples. For ease of reading, the BAc of clean DNN is referred as oBAc (original Benign Accuracy). Noise level γ is used to evaluate stealthiness. During evaluation, higher ASR, lower γ , and smaller reduction of BAc mean better backdoor pattern.

Attack Setting: For each victim 3D DNN, we follow its default setting in training and testing stage. The only change is the poisoned samples in D_{train} and their labels. The target class y^t is set to be 1 for every dataset and keep consistent with that of the comparison algorithms. Besides, the injection rate α is set to be 0.05, and the total D_{test} is used to generate poison testing data D_{test}^{poi} to evaluate ASR. For rotation noise level γ , it is a trade-off between ASR and stealthiness. In the experiment, we adjust it empirically. Besides, there are two hyper-parameters in our algorithm which are iteration times K and candidate noises number M . We set $K = 5$ and $M = 20$, and the reason will be illustrated in **Ablation Study**.

Compared Backdoor Attacks: We are the first backdoor attack that adapt for 3D mesh so far, hence, we mainly obvious *NRBdoor*'s ASR and stealthiness on 3D mesh. For point cloud, we compare *NRBdoor* with PointBA [30] and PointBA_X [31] which are SOTA backdoor attack methods. In detail, PointBA_X implants backdoor by adding a ball near the benign point cloud. Meanwhile, PointBA implants backdoor by two different patterns which are interaction pattern (PointBAi) and orientation pattern (PointBAo). In the experiments, we directly utilize their given results for comparison.

TABLE 1

Performance on Cubes. *NRBdoor* achieves perfect ASR when BAc reductions are less than 0.5% and stealthiness is guaranteed, shown as Fig 4.

Victim	<i>oBAc</i>	BAc	ASR	γ
MeshCNN	92.16	92.56	100	0.4
SubdivNet	100	100	100	0.9
MeshWalker	98.60	98.48	100	0.4

TABLE 2

Performance on Manifold40. ASR for three victim mesh DNNs are higher than 97%, and BAc reductions are less than 1%.

Victim	<i>oBAc</i>	BAc	ASR	γ
MeshNet	88.40	91.00	100	0.9
SubdivNet	91.22	91.02	99.13	0.8
MeshWalker	90.5	89.79	97.22	0.9

TABLE 3

Performance on Shrec16. The backdoor pattern is harder to be implanted than above two datasets due to the small data size.

Victim	<i>oBAc</i>	BAc	ASR	γ
MeshCNN	98.60	97.50	98.82	2.2
MeshNet	90	86.67	96.72	1.2
DiffusionNet	100	100	86.66	2.0

TABLE 4

Performance for Point Cloud on ModelNet40. *NRBdoor* achieves competitive ASR compared with PointBAi [30], PointBAo [30] and PointBA_X [31]. Here, **99.3** and **97.4** means the largest and second largest value respectively.

Victim	<i>oBAc</i>	BAc	ASR				γ
			<i>NRBdoor</i>	PointBAi	PointBAo	PointBA_X	
PointNet	89.20	84.15	<u>97.4</u>	99.3	93.2	96.0	0.5
PointNet++	90.70	89.85	99.27	<u>98.6</u>	94.7	96.9	0.9
DGCNN	92.90	92.03	97.14	100	<u>97.5</u>	96.1	0.4

4.2 Main Results

Attack Effectiveness: Table 1, Table 2 and Table 3 show the attack performance for mesh DNNs on three datasets. For Cubes, the results suggest that ASR achieves 100% for three victim mesh DNNs. The mapping from *NRBdoor* to y^t is well learned by each mesh DNN. Meanwhile, their BAc decrease slightly (less than 0.2%), which suggests that implanting *NRBdoor* have few influences on victim mesh DNN. For Manifold40, *NRBdoor* achieves 100% ASR for MeshNet. Meanwhile, ASR for SubdivNet and Meshwalker are both larger than 97%. For Shrec16, we find that the attack is more difficult. Specifically, the rotation noise γ requires to be loosed to 2.2 to achieve ASR > 98.82%, by now, the pattern stealthiness is very weak. The possible reason is that *NRBdoor* will be hardly learned by relatively small size of poisoned samples.

For point cloud, the comparison results between *NRBdoor*, PointBAi [30], PointBAo [30] and PointBA_X [31] are shown in Table 4. The results suggest that ASR of *NRBdoor* is competitive, and the BAc reduction of PointNet++ and DGCNN are both smaller than 1%. Besides, PointBAi and PointBA_X do not work for 3D mesh due to attaching

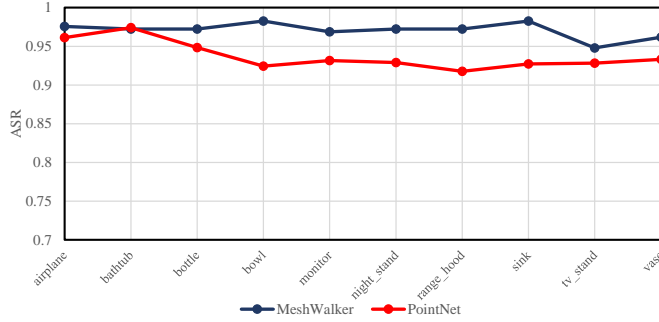


Fig. 3. Variation of ASR w.r.t. target class y^t for MeshWalker and PointNet on Manifold40 and ModelNet40 respectively. Results suggest that ASR is not sensitive to y^t .

a ball around a 3D mesh is forbidden in data structure. Meanwhile, although conducting PointBAo (clean rotation) on 3D mesh is allowed from the data format perspective, result from section 4.3 suggests that its average ASR is low (8.26%). Hence, *NRBdoor* achieves competitive ASR and wider application.

Furthermore, to evaluate the sensitivity of *NRBdoor* to target class y^t , we randomly select ten target classes from Manifold40 and ModelNet40 to test the ASR variation on 3D mesh and point cloud. Results in Fig 3 suggest that y^t have slightly influence on *NRBdoor*.

Attack Stealthiness: Fig 4 shows the poisoned 3D mesh from Cubes and Manifold40 with $ASR > 97\%$ on MeshCNN and MeshWalker. We find that the appearance of poisoned mesh by *NRBdoor* has slightly difference from the original. The most obvious change is a small orientation disparity caused by additional rotation, which it is a common operation in reality and is hard to get defender’s attention. For Cubes, the appearance variation is more obvious. The reason is that their original appearance is a regular cube, and thus a small disturbance tends to attract visual attention.

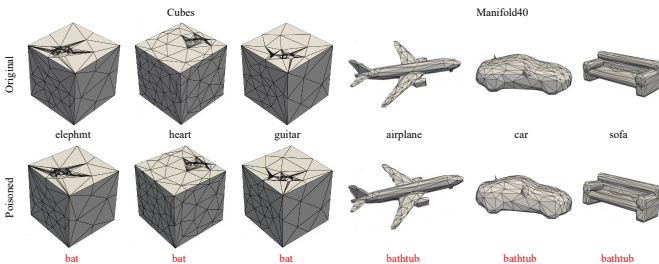


Fig. 4. 3D meshes poisoned by *NRBdoor* with $ASR > 97\%$. The shape variation is hard to be detected.

Moreover, Fig 5 exhibits the shape variation of point cloud after conducting four different backdoor patterns including PointBAi [30], PointBAo [30], PointBA_X [31] and *NRBdoor*. Specifically, PointBAi and PointBA_X are two similar backdoor patterns which implanted by adding a ball. Though, the two similar pattern do not change the point cloud itself, adding a ball around the object appears strange. In contrast, in spite of *NRBdoor* changes most points, the shape variation is few and is harder detected than PointBAi and PointBA_X. Therefore, *NRBdoor* is the most natural backdoor pattern.

At the same time, point clouds implanted by PointBAo are similar to point clouds implanted by *NRBdoor*, since PointBAo is conducted by clean rotation. However, in section 4.3, we prove that PointBAo is unable to implant backdoor into mesh DNN. Hence, *NRBdoor* is more widely used.

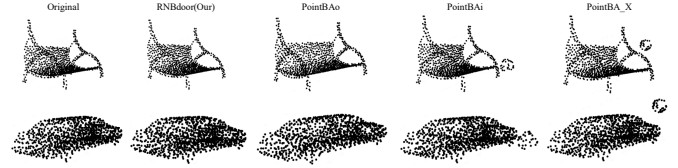


Fig. 5. Point cloud poisoned by PointBAi [30], PointBAo [30], PointBA_X [31] and *NRBdoor*. *NRBdoor* is more natural visually.

4.3 Necessity for Adding Noise

To prove it is necessary to add noisy on clean rotation, we implant clean rotation into MeshCNN to test attack performance. In detail, we randomly generate ten clean rotations as the backdoor pattern, and observe their ASR for comparing. Result suggests that the average, minimal and maximal ASR of the ten clean rotations are 8.26%, 4.55% and 12.88% respectively, which are lower than *NRBdoor*. Furthermore, Fig 6 shows 3D meshes poisoned by four random clean rotations and *NRBdoor*, which suggests that *NRBdoor* is more imperceptible and more powerful. Hence, adding noise to clean rotation is necessary to achieve high ASR.

Not that, the generated rotations include the orientation pattern used in PoinBA (PointBAo). Therefore, the results can also prove that PoinBAo is unable to implant backdoor into mesh DNN.

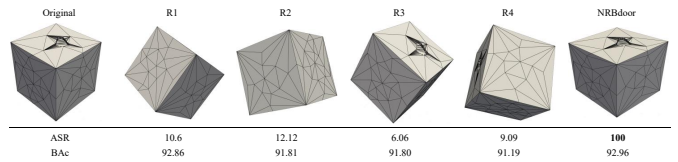


Fig. 6. Necessity for adding noise. Clean rotation can not implant backdoor into mesh DNN, in contrast, adding small noise to clean unit rotation acquires 100% ASR. In this figure, R1 means 1-st random rotation, and so on.

4.4 Ablation Study

To further understand *NRBdoor*, we conduct ablation experiments towards rotation noise level γ , poison rate α , iteration times K and candidate noises number M . MeshCNN is selected as the victim 3D DNN, and Cubes as the verifying datasets.

Noise Level γ is an important factor of our algorithm. It impacts ASR and stealthiness at the same time. Fig 7(a) suggests that $\gamma = 0.4$ is the optimal under $\alpha = 0.05$, since ASR is high and shape variation is small (shown as Fig 4). However, the optimal γ is different for each 3D DNN and datasets due to disparity data size and DNN structure. In addition, we find that BAe decreases when $\gamma < 0.3$. The possible reason is that the conducted poison is too slight

TABLE 5
Increasing Iteration Times K and Candidate Noises Number M will enlarge search space, and find better pattern.

K	1	3	5	7
ASR	85.00	91.35	100	100
BAC	91.61	91.73	92.30	91.85
M	5	10	15	20
ASR	80.00	85.00	97.5	100
BAC	91.73	91.61	91.65	92.50

to cause enough feature variation. Then, injecting poisoned samples is equal to fusing samples from different classes which will prevent 3D DNN from extracting unique feature for one certain class.

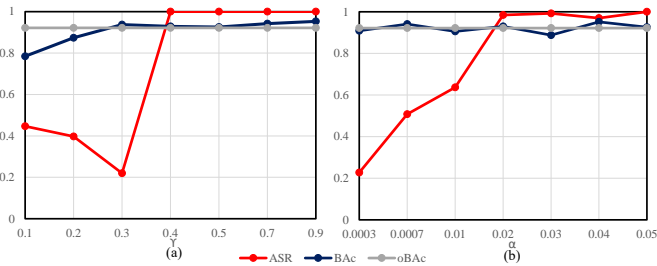


Fig. 7. Impact of γ and α . Higher γ brings higher ASR under $\gamma < 0.4$. Once $\gamma \geq 0.4$ ASR remains at 100%. Meanwhile, larger α provides more poisoned samples to enable 3D DNN to learn backdoor feature.

Poison Rate α : Fig 7(b) shows the variation of ASR and BAC w.r.t $0.003 < \alpha < 0.05$ under $\gamma = 0.5$. We find that ASR grows up along with α under $\alpha < 0.02$ and achieves 100% once $\alpha \geq 0.02$. At the same time, the reduction of BAC is small, which indicates a wonderful results. Hence, we can naturally give the conclusion that higher poison rate of *NRBdoor* leads to higher ASR.

Iteration Times K : To better visualize ASR variation tendency along with K and M , we set $\gamma = 0.4$ and $\alpha = 0.05$ for study. Table 5 shows the ASR tendency according to iteration times K , which suggests that more iteration times is able to find better pattern and achieve higher ASR.

Candidate Noises Number M determines the search space of our algorithm. As shown in table 5, ASR increases along with M increases. The reason is that larger M brings better pattern diversity.

4.5 Resistance to Defender

Data Augmentation: In 2D and 3D domain, data augmentation is a popular method to increase DNN robustness. To verify whether it can be resisted by *NRBdoor*, we apply random rotation and scaling for data augmentation in training stage. The victim 3D DNNs are PointNet and MeshCNN. Experiment results suggest that ASR of two 3D DNNs slightly decrease 5% for both random rotation and scaling.

Saliency-based Defense: Up to now, there is few baseline method for defending backdoor attack on point cloud or 3D mesh. In detail, [55] is specifically designed for points attaching based attack like PointBA_X, and will be technically disable for *NRBdoor*. Hence, we follow the popular

defense way in image domain [56], [57] and extend them to point cloud. They detect the backdoor pattern by searching for critical regions from input towards each class utilizing saliency map technique.

The critical issue for extending them to point cloud is how to build point cloud saliency map. Here, we utilize the method from [58], which is the first work to research point cloud saliency. The author expresses points in spherical coordinate system. By this way, shifting a point towards the center by η will increase the loss L by $-\frac{dL}{dr}\eta$:

$$\frac{dL}{dr_i} = \sum_{j=1}^3 \frac{dL}{dx_{ij}} \frac{x_{ij} - x_{cj}}{r_i} \quad (12)$$

Where, $r_i = \sqrt{\sum_{j=1}^3 (x_{ij} - x_{cj})^2}$, x_c is the point cloud center, x is the euclidean coordinates of each point. Furthermore, to allow more flexibility in saliency map construction, the author applies a change-of-variable by $\rho_i = r_i^{-\beta}$, where β is a hyper parameter. Thus, the saliency score of point i is:

$$s_i = -\frac{dL}{dr_i} r_i^{1+\beta} \quad (13)$$

Saliency map reveals the points 3D DNN focuses on when making its decision. Higher saliency score represents higher importance. Moreover, backdoor pattern in point cloud is the major portion one infected 3D DNN focuses on. Therefore, we utilize saliency score to detect and drop the backdoor pattern for defense. The designed Saliency-based Point cloud backdoor defense (SP-defense) can be described as: 1) calculate saliency score s_i by equation (13) for every point, 2) locate backdoor pattern by ranking q highest score points, 3) drop the detected pattern for defense.



Fig. 8. Red points represent the detected backdoor pattern by SP-defense. Results show that the backdoor pattern implanted by PointBA_X is well detected by SP-defense. In contrast, *NRBdoor* can evade to SP-defense.

We defend PointBA_X and *NRBdoor* by the designed SP-defense under $q = 35, \beta = 1$. For PointBA_X, we follow its original setting. In detail, the original classes are *flower_pot, cone, bottle, chair, wardrobe, guitar* and target class y^t is *toilet*, the local geometric of backdoor pattern is RS: 32 points randomly distributed on a sphere. PointNet and ModelNet40 are selected as the victim model and the verifying dataset respectively.

Fig 8 exhibits that the injected pattern by PointBA_X can be well detected by SP-defense. In contrast, *NRBdoor* is immune to SP-defense, since the pattern is conducted on total point cloud instead of specified point sets. Meanwhile, ASR of *NRBdoor* marginally decreases from 93.44% to 88.39%,

in contrast, ASR of PointBA_X decreases from 89.40% to 25.40%.

5 CONCLUSIONS

This paper proposes the first uniform backdoor pattern: *NRBdoor* for 3D shape. *NRBdoor* is constructed by a common operation in 3D world, which is noisy rotation, hence it is natural and imperceptible. *NRBdoor* achieves 100% ASR in many cases and is able to adapt for data structure variation during implanting backdoor into 3D DNN. At the same time, it is the first work to implant backdoor into mesh DNN. In the end, we design a backdoor defense method based on saliency map theory named SP-defense. It can reduce ASR of PointBA_X from 82% to 23%, but has very little effect on our *NRBdoor*.

REFERENCES

- [1] Di Wang, Lulu Tang, Xu Wang, Luqing Luo, and Zhi-Xin Yang. Improving deep learning on point cloud by maximizing mutual information across layers. *Pattern Recognition*, 131:108892, 2022.
- [2] Ilyass Abouelaziz, Aladine Chetouani, Mohammed El Hassouni, Longin Jan Latecki, and Hocine Cherifi. No-reference mesh visual quality assessment via ensemble of convolutional neural networks and compact multi-linear pooling. *Pattern Recognition*, 100:107174, 2020.
- [3] Jinwon Lee, Hyunoh Lee, and Duhwan Mun. 3d convolutional neural network for machining feature recognition with gradient-based visual explanations from 3d cad models. *Scientific Reports*, 12(1):1–14, 2022.
- [4] Hyunoh Lee, Jinwon Lee, Hyunki Kim, and Duhwan Mun. Dataset and method for deep learning-based reconstruction of 3d cad models containing machining features for mechanical parts. *Journal of Computational Design and Engineering*, 9(1):114–127, 2022.
- [5] Vincent A Cicirello and William C Regli. A flexible and extensible approach to automated cad/cam format classification. *Computers & graphics*, 37(5):484–495, 2013.
- [6] Alex Krizhevsky, Ilya Sutskever, and Geoffrey E Hinton. Imagenet classification with deep convolutional neural networks. *Communications of the ACM*, 60(6):84–90, 2017.
- [7] Sergey Ioffe and Christian Szegedy. Batch normalization: Accelerating deep network training by reducing internal covariate shift. In *International conference on machine learning*, pages 448–456. PMLR, 2015.
- [8] Karen Simonyan and Andrew Zisserman. Very deep convolutional networks for large-scale image recognition. *arXiv preprint arXiv:1409.1556*, 2014.
- [9] Rana Hanocka, Amir Hertz, Noa Fish, Raja Giryes, Shachar Fleishman, and Daniel Cohen-Or. Meshcnn: a network with an edge. *ACM Transactions on Graphics (TOG)*, 38(4):1–12, 2019.
- [10] Nicholas Sharp, Souhaib Attaiki, Keenan Crane, and Maks Ovsjanikov. Diffusionnet: Discretization agnostic learning on surfaces. *ACM Transactions on Graphics (TOG)*, 41(3):1–16, 2022.
- [11] Shi-Min Hu, Zheng-Ning Liu, Meng-Hao Guo, Jun-Xiong Cai, Jiahui Huang, Tai-Jiang Mu, and Ralph R Martin. Subdivision-based mesh convolution networks. *ACM Transactions on Graphics (TOG)*, 41(3):1–16, 2022.
- [12] Charles R Qi, Hao Su, Kaichun Mo, and Leonidas J Guibas. Pointnet: Deep learning on point sets for 3d classification and segmentation. In *Proceedings of the IEEE conference on computer vision and pattern recognition*, pages 652–660, 2017.
- [13] Yue Wang, Yongbin Sun, Ziwei Liu, Sanjay E Sarma, Michael M Bronstein, and Justin M Solomon. Dynamic graph cnn for learning on point clouds. *Acm Transactions On Graphics (tog)*, 38(5):1–12, 2019.
- [14] Xumin Yu, Lulu Tang, Yongming Rao, Tiejun Huang, Jie Zhou, and Jiwen Lu. Point-bert: Pre-training 3d point cloud transformers with masked point modeling. In *Proceedings of the IEEE/CVF International Conference on Computer Vision and Pattern Recognition*, pages 19313–19322, 2022.
- [15] Derui Wang, Chaoran Li, Sheng Wen, Surya Nepal, and Yang Xiang. Man-in-the-middle attacks against machine learning classifiers via malicious generative models. *IEEE Transactions on Dependable and Secure Computing*, 18(5):2074–2087, 2020.
- [16] Yiqi Zhong, Xianming Liu, Deming Zhai, Junjun Jiang, and Xiangyang Ji. Shadows can be dangerous: Stealthy and effective physical-world adversarial attack by natural phenomenon. In *Proceedings of the IEEE/CVF Conference on Computer Vision and Pattern Recognition*, pages 15345–15354, 2022.
- [17] Zhibo Wang, Mengkai Song, Siyan Zheng, Zhifei Zhang, Yang Song, and Qian Wang. Invisible adversarial attack against deep neural networks: An adaptive penalization approach. *IEEE Transactions on Dependable and Secure Computing*, 18(3):1474–1488, 2019.
- [18] Chaoran Li, Xiao Chen, Derui Wang, Sheng Wen, Muhammad Ejaz Ahmed, Seyit Camtepe, and Yang Xiang. Backdoor attack on machine learning based android malware detectors. *IEEE Transactions on Dependable and Secure Computing*, 2021.
- [19] Ian J Goodfellow, Jonathon Shlens, and Christian Szegedy. Explaining and harnessing adversarial examples. *arXiv preprint arXiv:1412.6572*, 2014.
- [20] Aleksander Madry, Aleksandar Makelov, Ludwig Schmidt, Dimitris Tsipras, and Adrian Vladu. Towards deep learning models resistant to adversarial attacks. *arXiv preprint arXiv:1706.06083*, 2017.
- [21] Abdullah Hamdi, Sara Rojas, Ali Thabet, and Bernard Ghanem. Advpc: Transferable adversarial perturbations on 3d point clouds. In *European Conference on Computer Vision*, pages 241–257. Springer, 2020.
- [22] Huangxin Xu, Fazhi He, Linkun Fan, and Junwei Bai. D3adv: A direct 3d adversarial sample attack inside mesh data. *Computer Aided Geometric Design*, 97:102122, 2022.
- [23] Lei Bu, Zhe Zhao, Yuchao Duan, and Fu Song. Taking care of the discretization problem: A comprehensive study of the discretization problem and a black-box adversarial attack in discrete integer domain. *IEEE Transactions on Dependable and Secure Computing*, 2021.
- [24] Xurong Li, Shouling Ji, Meng Han, Juntao Ji, Zhenyu Ren, Yushan Liu, and Chunming Wu. Adversarial examples versus cloud-based detectors: A black-box empirical study. *IEEE Transactions on Dependable and Secure Computing*, 18(4):1933–1949, 2019.
- [25] Jiancheng Yang, Qiang Zhang, Rongyao Fang, Bingbing Ni, Jinxian Liu, and Qi Tian. Adversarial attack and defense on point sets. *arXiv preprint arXiv:1902.10899*, 2019.
- [26] Sizhe Chen, Zhengbao He, Chengjin Sun, Jie Yang, and Xiaolin Huang. Universal adversarial attack on attention and the resulting dataset damagenet. *IEEE Transactions on Pattern Analysis and Machine Intelligence*, 2020.
- [27] Zichao Hu, Heng Li, Liheng Yuan, Zhang Cheng, Wei Yuan, and Ming Zhu. Model scheduling and sample selection for ensemble adversarial example attacks. *Pattern Recognition*, page 108824, 2022.
- [28] Emily Wenger, Josephine Passananti, Arjun Nitin Bhagoji, Yuan-shun Yao, Haitao Zheng, and Ben Y Zhao. Backdoor attacks against deep learning systems in the physical world. In *Proceedings of the IEEE/CVF Conference on Computer Vision and Pattern Recognition*, pages 6206–6215, 2021.
- [29] Shan Jia, Guodong Guo, and Zhengquan Xu. A survey on 3d mask presentation attack detection and countermeasures. *Pattern recognition*, 98:107032, 2020.
- [30] Xinke Li, Zhirui Chen, Yue Zhao, Zekun Tong, Yabang Zhao, Andrew Lim, and Joey Tianyi Zhou. Pointba: Towards backdoor attacks in 3d point cloud. In *Proceedings of the IEEE/CVF International Conference on Computer Vision*, pages 16492–16501, 2021.
- [31] Zhen Xiang, David J Miller, Siheng Chen, Xi Li, and George Kesidis. A backdoor attack against 3d point cloud classifiers. In *Proceedings of the IEEE/CVF International Conference on Computer Vision*, pages 7597–7607, 2021.
- [32] Mingfu Xue, Can He, Jian Wang, and Weiqiang Liu. One-to-n & n-to-one: Two advanced backdoor attacks against deep learning models. *IEEE Transactions on Dependable and Secure Computing*, 2020.
- [33] Tianyu Gu, Kang Liu, Brendan Dolan-Gavitt, and Siddharth Garg. Badnets: Evaluating backdooring attacks on deep neural networks. *IEEE Access*, 7:47230–47244, 2019.
- [34] Yunfei Liu, Xingjun Ma, James Bailey, and Feng Lu. Reflection backdoor: A natural backdoor attack on deep neural networks. In

- European Conference on Computer Vision*, pages 182–199. Springer, 2020.
- [35] Yiming Li, Tongqing Zhai, Yong Jiang, Zhifeng Li, and Shu-Tao Xia. Backdoor attack in the physical world. *arXiv preprint arXiv:2104.02361*, 2021.
- [36] Shaofeng Li, Minhui Xue, Benjamin Zi Hao Zhao, Haojin Zhu, and Xinpeng Zhang. Invisible backdoor attacks on deep neural networks via steganography and regularization. *IEEE Transactions on Dependable and Secure Computing*, 18(5):2088–2105, 2020.
- [37] Yuezun Li, Yiming Li, Baoyuan Wu, Longkang Li, Ran He, and Siwei Lyu. Invisible backdoor attack with sample-specific triggers. In *Proceedings of the IEEE/CVF International Conference on Computer Vision*, pages 16463–16472, 2021.
- [38] Fan Lu, Guang Chen, Sanqing Qu, Zhijun Li, Yinlong Liu, and Alois Knoll. Pointinet: Point cloud frame interpolation network. In *Proceedings of the AAAI Conference on Artificial Intelligence*, volume 35, pages 2251–2259, 2021.
- [39] Innfarn Yoo, Huiwen Chang, Xiyang Luo, Ondrej Stava, Ce Liu, Peyman Milanfar, and Feng Yang. Deep 3d-to-2d watermarking: Embedding messages in 3d meshes and extracting them from 2d renderings. In *Proceedings of the IEEE/CVF Conference on Computer Vision and Pattern Recognition*, pages 10031–10040, 2022.
- [40] Charles Ruizhongtai Qi, Li Yi, Hao Su, and Leonidas J Guibas. Pointnet++: Deep hierarchical feature learning on point sets in a metric space. *Advances in neural information processing systems*, 30, 2017.
- [41] Meng-Hao Guo, Jun-Xiong Cai, Zheng-Ning Liu, Tai-Jiang Mu, Ralph R Martin, and Shi-Min Hu. Pct: Point cloud transformer. *Computational Visual Media*, 7(2):187–199, 2021.
- [42] Ayellet Lahav, Alon Tal. Meshwalker: Deep mesh understanding by random walks. *ACM Transactions on Graphics (TOG)*, 39(6):1–13, 2020.
- [43] Yiming Li, Yong Jiang, Zhifeng Li, and Shu-Tao Xia. Backdoor learning: A survey. *IEEE Transactions on Neural Networks and Learning Systems*, 2022.
- [44] Shihao Zhao, Xingjun Ma, Xiang Zheng, James Bailey, Jingjing Chen, and Yu-Gang Jiang. Clean-label backdoor attacks on video recognition models. In *Proceedings of the IEEE/CVF Conference on Computer Vision and Pattern Recognition*, pages 14443–14452, 2020.
- [45] Liang Chen, Qibiao Peng, Jintang Li, Yang Liu, Jiawei Chen, Yong Li, and Zibin Zheng. Neighboring backdoor attacks on graph convolutional network. *arXiv preprint arXiv:2201.06202*, 2022.
- [46] Guiyu Tian, Wenhao Jiang, Wei Liu, and Yadong Mu. Poisoning morphnet for clean-label backdoor attack to point clouds. *arXiv preprint arXiv:2105.04839*, 2021.
- [47] Bo Chen, Alvaro Parra, Jiewei Cao, Nan Li, and Tat-Jun Chin. End-to-end learnable geometric vision by backpropagating pnp optimization. In *Proceedings of the IEEE/CVF Conference on Computer Vision and Pattern Recognition*, pages 8100–8109, 2020.
- [48] Xiao-Shan Gao, Xiao-Rong Hou, Jianliang Tang, and Hang-Fei Cheng. Complete solution classification for the perspective-three-point problem. *IEEE transactions on pattern analysis and machine intelligence*, 25(8):930–943, 2003.
- [49] Vincent Moreno-Noguer Lepetit. Eppn: An accurate o (n) solution to the pnp problem. *International journal of computer vision*, 81(2):155–166, 2009.
- [50] Yanyan Li, Shiyue Fan, Yanbiao Sun, Qiang Wang, and Shanlin Sun. Bundle adjustment method using sparse bfgs solution. *Remote Sensing Letters*, 9(8):789–798, 2018.
- [51] Neil D Besl, Paul J McKay. Method for registration of 3-d shapes. In *Sensor fusion IV: control paradigms and data structures*, volume 1611, pages 586–606. Spie, 1992.
- [52] Z Lian, A Godil, B Bustos, M Daoudi, J Hermans, S Kawamura, Y Kurita, G Lavoua, P Dp Suetens, et al. Shape retrieval on non-rigid 3d watertight meshes. In *Eurographics workshop on 3d object retrieval (3DOR)*. Citeseer, 2011.
- [53] Yutong Feng, Yifan Feng, Haoxuan You, Xibin Zhao, and Yue Gao. Meshnet: Mesh neural network for 3d shape representation. In *Proceedings of the AAAI Conference on Artificial Intelligence*, volume 33, pages 8279–8286, 2019.
- [54] Zhirong Wu, Shuran Song, Aditya Khosla, Fisher Yu, Linguang Zhang, Xiaoou Tang, and Jianxiong Xiao. 3d shapenets: A deep representation for volumetric shapes. In *Proceedings of the IEEE conference on computer vision and pattern recognition*, pages 1912–1920, 2015.
- [55] Zhen Xiang, David J Miller, Siheng Chen, Xi Li, and George Kesidis. Detecting backdoor attacks against point cloud classifiers. In *ICASSP 2022-2022 IEEE International Conference on Acoustics, Speech and Signal Processing (ICASSP)*, pages 3159–3163. IEEE, 2022.
- [56] Florian Pellegrino Chou, Edward Tramer. Sentinet: Detecting localized universal attacks against deep learning systems. In *2020 IEEE Security and Privacy Workshops (SPW)*, pages 48–54. IEEE, 2020.
- [57] Moustafa Srivastava Huang, Xijie Alzantot. Neuroninspect: Detecting backdoors in neural networks via output explanations. *arXiv preprint arXiv:1911.07399*, 2019.
- [58] Tianhang Zheng, Changyou Chen, Junsong Yuan, Bo Li, and Kui Ren. Pointcloud saliency maps. In *Proceedings of the IEEE/CVF International Conference on Computer Vision*, pages 1598–1606, 2019.